THE PENNSYLVANIA STATE UNIVERSITY
SCHREYER HONORS COLLEGE

DEPARTMENT OF BIOMEDICAL ENGINEERING

CHARACTERIZATION OF ANTICANCER LECTINS AND DEVELOPMENT OF NANOGEL-BASED CARRIERS FOR THEIR TARGETED DELIVERY

ATIP LAWANPRASERT
SPRING 2018

A thesis
submitted in partial fulfillment
of the requirements
for a baccalaureate degree
in Biomedical Engineering
with honors in Biomedical Engineering

Reviewed and approved* by the following:

Scott H. Medina
Assistant Professor of Biomedical Engineering
Thesis Adviser

Jian Yang
Professor of Biomedical Engineering
Honors Adviser

* Signatures are on file in the Schreyer Honors College.

ABSTRACT

Glycans are covalently-linked carbohydrates displayed from the surface of mammalian cells, which play critical roles in a variety of cellular biological functions. Dysregulation of glycan processing in cells is also involved in many human diseases, including cancer. Thus, molecules that can distinguish mammalian and cancer-specific glycans represent new tools to diagnose and treat cancer. One such class of agents is lectins, which represent a family of carbohydrate-binding proteins that recognize glycans with high specificity. Importantly, many lectins are able to modulate the functions of cells following glycan binding and thus represent attractive new therapeutic candidates in oncology. In the first chapter of my thesis I discuss our recent discovery of a new family of naturally-derived lectins, and detail their application in anticancer therapy and diagnosis. Despite the therapeutic potential of these new agents, protein-based drugs face a number of challenges that limit their clinical utility, including rapid degradation and off-target toxicity. As a result, drug delivery devices that protect protein cargo during delivery, and selectively localize it to cancerous tissues are urgently needed. Towards this goal, in the second chapter of my thesis I discuss the development of a new class of inhalable nanoparticle formed from the electrostatic cross-linking of FDA-approved biologic polymers: Poly(L-Lysine) (PLL) and hyaluronic acid (HA). Herein, we present recent work in the development and validation of these new nanoparticles for drug delivery applications, with a particular focus on protein delivery for lung cancer therapy.

TABLE OF CONTENTS

LIST OF FIGURES

LIST OF TABLES

ACKNOWLEDGEMENTS

Firstly, I would like to thank Dr. Scott H. Medina of the Penn State Biomedical Engineering Department for kindly providing advice and facilities in order to complete both projects. Moreover, I would like to thank Dr. James H. Marden of the Penn State Biology Department for kindly providing the necessary tools for completing the lectin characterization. Also, I would like to thank Andrew S. Simonson of the Penn State Biomedical Engineering for kindly assisting in the completion of the nanogel-based delivery method.

Chapter 1

Introduction of the Lectin-based therapy

Glycans

The outer surfaces of mammalian cells are decorated with a complex array of branched carbohydrate polymers attached to membrane proteins or lipids, collectively referred to as glycans (Lannoo, 2015). The structural diversity of these molecules leads to a broad spectrum of biological functions, where glycans play key roles in protein folding, modulation of immune responses and wound healing, to name a few. Dysregulation of glycosylation is also central to the initiation and progression of various human diseases. For example, the early stage of cancer development is characterized by changes in the normal glycosylation pathway resulting in the synthesis of abnormal glycan structures (Oliveira-Ferrer, 2017). Also, cancer cells are shown to possess a different set of genes from their original cells, thus leading to the synthesis of unique glycan structures that are often cancer-specific (Ishikawa, 2017).

Importantly, the glycan “fingerprint” of cancer can be used as a biomarker to identify malignant cells and the potential of signaling pathway disruption. This allows proteins capable of recognizing and binding distinct glycan structures to serve as new tools in precision medicine for the diagnosis and therapy of cancer. One such class of proteins are lectins.

Lectins

Lectins are family of carbohydrate-binding proteins that recognize and bind to mammalian glycans with high specificity, frequently resulting in modulating the activity of target cells (Liu, 2012). For example, ricin which is a ribosome-inactivating lectin, is produced in the seeds of the castor oil plant, (Chen, 2014). The median lethal dose of ricin is approximately 22 micrograms per kilogram of body weight (European Food Safety Authority, EFSA, 2008). Thus, the potency and high affinity of many lectins for their targets can cause significant biologic effects at low doses. In addition, lectins are also used in many medical diagnostic procedures. For instance, various types of lectins are used to screen glycoproteins/glycolipids in blood samples (Ghosh, 2016).

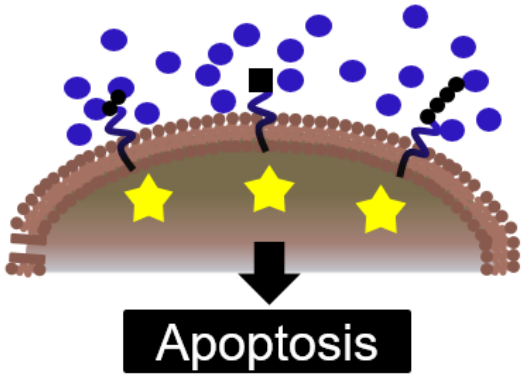

Figure 1. Lectins bind to glycans presented on mammalian cell surfaces with high specificity. Stimulation of cell surface receptors by lectins can alter cell signaling and trigger cell apoptosis.

Lectins also play a role in the human immune system. For instance, human mannose-binding lectin (hMBL) is used in the immune system to bind to the high-mannose glycoprotein coat of pathogenic microbes and apoptotic cells. As I report later in the thesis, we discovered a new MBL that displays potent anticancer activity toward mucosal tumor cell lines. Therefore for the purposes of this introduction I will limit the discussion to MBLs.

Mannose-Binding Lectins (MBL)

Mannose-binding lectins (MBL) are subset of lectins that play key roles in orchestrating innate immunity by the lectin pathway (Fraser, 1998) and can selectively recognize glycans displayed on cancer cells. Mannose-binding lectins are generally found in human blood serum. They are responsible for binding to pathogens, leading to immune signaling and clearance of the bacteria from the host. They also interact with aberrant cells and mediate cell destruction via apoptosis. This suggests MBLs may be able to serve as novel anticancer agents. In the ideal case, the MBL molecule binds specifically to cancer-associated glycans to induce programmed cell death (i.e. apoptosis) in the cancer cell. In particular, selective induction of apoptosis in cancer cells is an attractive strategy for therapy as it produces minimal cell debris, thus reducing local inflammation and collateral damage to nearby healthy cells (Elmore, 2007).

With this background in mind, I explored the biological activity of a family of lectins recently discovered by the Marden laboratory during functional genomic analyses of tropical rainforest tree root samples. The first lectin synthesized by the Marden Lab, "**Lectin-1**", contains six mannose-binding domains, suggesting that it may be able to avidly coordinate with mannose residues on the cell surface to elicit toxicity. A subsequent collaboration between the Marden and Medina laboratories, housed in the Penn State Biomedical Engineering Department, afforded me the opportunity to screen **Lectin 1** with a small library of cancer cell lines to characterize its potential to be used as a protein-based anticancer therapy. These studies are described in Chapter 2 of this thesis.

Cell-lines and the nature of *in vitro* studies

In vitro cell-viability assays are convenient methods to rapidly screen potential anticancer compounds and assess their cytotoxic potential. These assays are relatively inexpensive, easy to perform, and serve as a convenient initial model before studying tumor biology in an animal model. Similar studies in non-malignant cell lines can be used to assess the specificity and biocompatibility of the tested lectins. The selected cell lines from various cell origins are shown in **Table 1**.

Table 1. The selected cell lines from various cell origins and types of cells

Cell lines	Cell origins	Note
Jurkat	Blood (T-lymphocyte)	Suspension cell
MCF-7	Breast cancer	Cancer cell
HeLa	Cervical cancer	Cancer cell, mucous cell
A549	Lung cancer	Cancer cell, mucous cell
OVCAR-3	Ovary cancer	Cancer cell, mucous cell
T24	Urinary bladder cancer	Cancer cell, Mucous cell
CACO-2	Colon cancer	Cancer cell, Mucous cell
HDF	Human dermal fibroblast	Non-malignant cell

The selected cell lines should be suitable to provide initial insight into Lectin 1 activity, particularly the selectivity. Despite the therapeutic potential of the lectins, protein-based therapeutics suffer from a number of challenges that can limit their clinical utility. These include: 1) Rapid degradation in the circulatory system by serum proteases; 2) Poor distribution into the tumor tissues; 3) Off-target toxicity towards healthy cells; and 4) Potential non-specific stimulation of the immune system leading to systemic inflammation. To overcome these limitations, new protein-based therapeutics with novel delivery platforms must be explored to protect the biologic cargo during circulation as well as precisely deliver the cargo to tumor tissues. More details regarding the limitations of protein-therapeutics, and the proposed potential technologies to circumvent these issues, are presented in Chapter 4 of this theis.

Chapter 2

Lectin Experiments - Materials and Methods

Chemicals

These following chemicals were used in this study:

Annexin-V/PI staining kit (BD Bioscience, San Jose, CA), dimethyl sulfoxide (DMSO cell culture grade, Fisher BioReagents, Bellefonte, PA), DMSO spectrophotometric-grade (Alfa Aesar, Haverhill, MA),). doxorubicin hydrochloride (Oakwood Chemicals, Estill, SC), DMEM, fetal bovine serum, L-glutamine (Corning, NY), GFP (kindly provided by the National Institutes of Health, Rockville, MD), gentamycin (VWR, Radnor, PA), hyaluronic acid high molecular weight (Lifecore Biomedical, Chaska, MN), Lectin 1 (kindly provided by Dr. James Marden laboratory, University Park, PA), LSGS and Medium-106 (Thermo Fisher Scientific, Bellefonte, PA), MTT (Chem-Impex International, Wood Dale, IL), 0.1% w/v Poly(L-Lysine) solution (Alamanda Polymers, Huntsville, AL), phosphate buffer saline, RPMI-1640 (Corning, NY), trypsin solution (Corning, NY).

Cell culture

A549, HeLa, Jurkat, CACO-2, MCF-7, OVCAR-3, NCI/ADR-RES and T24 cell lines were kindly provided by the National Cancer Institute (Rockville, MD). HDF cell line was kindly provided by Dr. Yong Wang's laboratory of the Penn State Biomedical Engineering Department.

Complete growth media for A549, HeLa, Jurkat, MCF-7, OVCAR-3, NCI/ADR-RES and T24 cell lines comprised 0.1% gentamycin, 1% L-glutamine, and 10% fetal bovine serum in RPMI-1640. CACO-2 cell line complete growth media comprised 0.1% gentamycin, 1% L-glutamine, and 10% fetal bovine serum in DMEM. HDF cell line complete growth media comprised 2% low serum growth supplements in Medium-106. Cells were incubated in 37 degree Celsius, 5% CO_2, and high humidity incubator.

Cell viability assay

A549, HeLa, Jurkat, and T24 cell lines were seeded into 96-well plate at the concentration of 2000 cells/well. MCF-7, OVCAR-3, CACO-2, and HDF cell lines were seeded into 96-well plate at the concentration of 5000 cells/well. Cells were incubated in 37 degree Celsius and 5% CO_2 incubator for 24 hours before treatments. The supernatant was removed before treatments. Lectin 1 was prepared by serial dilution. The concentrations were varied based on the preliminary screening. For A549, CACO-2, HeLa, OVCAR-3, and T24, Lectin 1 concentration determined were ranged from $3x10^{-10}$ mg/mL to $3x10^{-5}$ mg/mL with the serial dilution factor of 10. For Jurkat and MCF-7 cell lines, concentrations of Lectin 1 were ranged from 3 mg/mL to $3x10^{-5}$ mg/mL with the serial dilution factor of 10. The negative control was performed using complete media while 20% DMSO in the complete media was used in the positive control. The final volume of solution in each well during treatment was 100 uL/well. Cells were incubated in 37 degree Celsius, 5% CO_2 condition for 48 hours. After that, the supernatant was removed and 0.5 mg/mL MTT in complete media solution was added to each well. The MTT-added plate was incubated for 2 hours. Then the supernatant was removed and 100 uL of spectrophotometry-grade DMSO was added to each well. The plate wasincubated for 15 minutes. Finally, the absorbance was determined at 540 nm using the microplate reader (BioTek; Winooski, VT).

The absorbance value was normalized to the untreated control with the subtraction of background from the positive control. The % viability value for each Lectin 1 concentration was calculated by the equation as followed:

$$\%\ Cell\ viability = \frac{Treated\ absorbance - background}{Untreated\ absorbance - background} * 100\%$$

Statistical analysis

For cell cytotoxicity assays, the data was presented as mean ± SD from at least three independent experiments. Difference between 2 groups was determined using *t* -test with 2-tails assuming unequal variances. The difference of mean among multiple concentrations of the treatments was determined by ANOVA followed by Dunnett's test. The level of significance was determined as $p < 0.05$.

For the controlled release experiments, the data was presented as mean ± SD from at least three independent runs.

Chapter 3

Results – Characterization of Lectin 1

Lectin 1: Cytotoxicity on cancer cells

Preliminary *in vitro* cytotoxicity shows that Lectin 1 had high potency towards certain cancer cell lines, including HeLa, A549, OVCAR-3, T24, and CACO-2 **(Figure 2)**. Interestingly, all of these cell lines are of a mucosal origin, suggesting Lectin 1 may show selective cancer therapy towards mucosal tumor tissue which is characterized by a heavily glycosylated cell surface (Varki A, 2009). Conversely, Lectin-1 was not active towards the non-mucosal MCF-7 and Jurkat cancer cell lines, or the non-malignant control line human dermal fibroblasts (HDF). IC_{50} values were calculated and are shown in the **Table 2.**

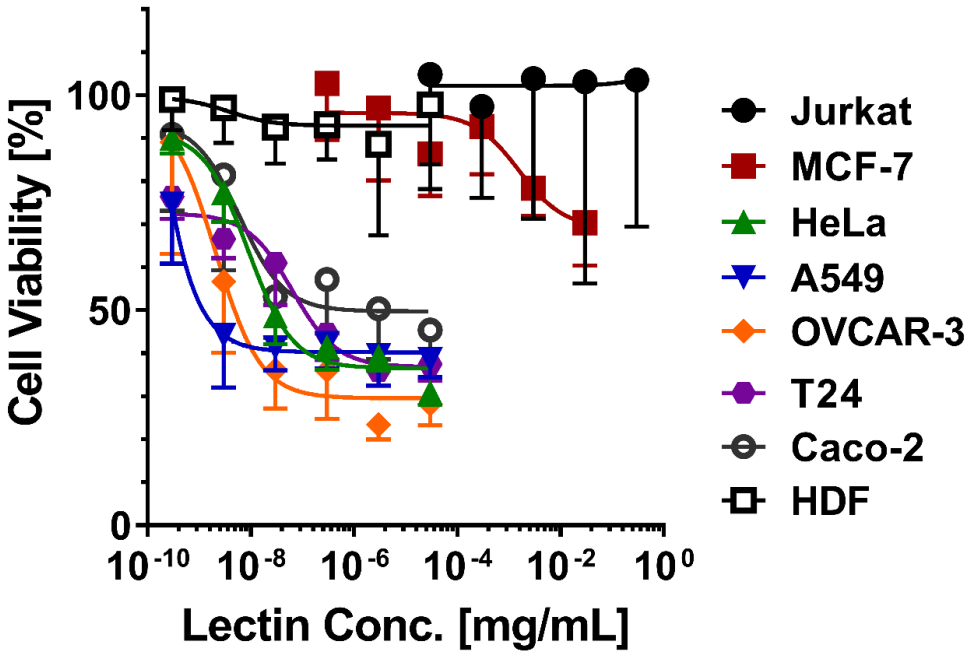

Figure 2. Cell viability curves of each cell lines treated with Lectin 1. The results were read at 48 hours after the treatments were added at each concentration.

Microscopy images of selected cell lines treated by Lectin 1 at 24 hours are shown in **Figure 3**. A549 and HeLa cells, which are sensitive to Lectin 1, show significantly changed cell morphologies. Here, cells are rounded and do not show a typical spread morphology, indicating potential apoptosis. Meanwhile, MCF-7 cells, which were insensitive to the lectin, did not show a change in morphology when treated.

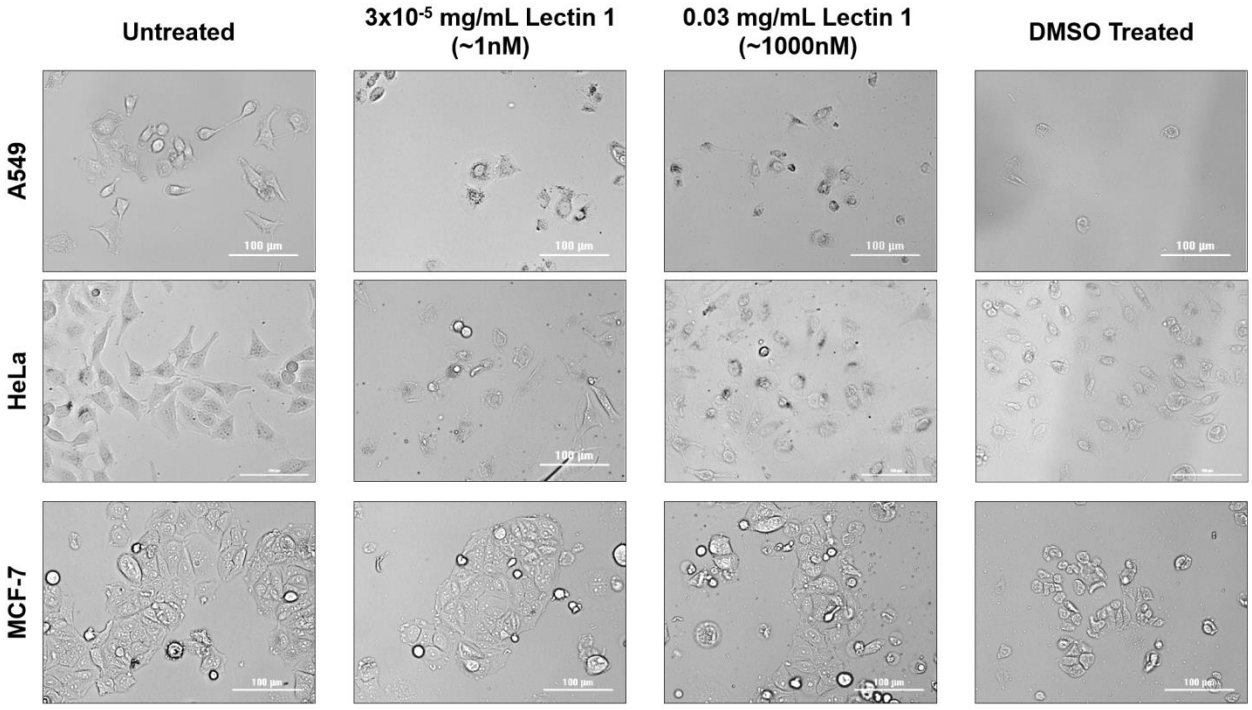

Figure 3. Microscopic images of A549, HeLa and MCF-7 cells 1 hour after treatment with Lectin 1 at two selected concentrations. Untreated cells, or those killed using 20% DMSO, are show as negative and positive controls, respectively.

The IC_{50} values (**Table 2**) were calculated based on the viability results as shown above (**Figure 2**). The lowest $IC_{50,}$ which determines the highest potency of Lectin, was at 0.05 pM in the A549 lung carcinoma cell line. OVCAR-3, HeLa, T24, and CACO-2 cells also displayed significant sensitivity to the lectin, as characterized by low picomolar IC_{50} values.

Table 2. Calculated IC_{50} values for each cell lines treated with Lectin 1 at 48 hours.

Lectin 1 Activity		
Cell Line	**IC_{50} [mg/mL]**	**IC_{50} [pM]**
A549	1.2×10^{-9}	0.04
OVCAR-3	4.9×10^{-9}	0.18
HeLa	2.6×10^{-8}	0.93
T24	1.1×10^{-7}	3.93
Caco-2	6.7×10^{-7}	23.93
MCF-7	>0.03	1.07×10^{6}
Jurkat	>0.03	1.07×10^{6}

These extremely promising results suggest that Lectin 1 may serve as a potent and highly selective therapeutic, particularly towards lung tumors (see A549 data above). While encouraging, protein-based therapies face a number of clinical hurdles, including rapid serum, poor tumor biodistribution and off-target toxicity. Thus, developing new anticancer proteins, like Lectin 1, towards clinical applications requires complimenting their discovery with novel delivery modalities. In the next chapter we present work on a new delivery vehicle for protein therapies.

Chapter 4

Introduction to nanogel carrier for targeted protein delivery

Challenges to protein-based oncology

Protein-based drugs face multiple threats inside our body (Frokjaer, 2005). The first obstacle is enzymatic degradation of the foreign biologic by serum proteases. Binding of plasma proteases with the protein-based drug results in hydrolysis of the peptide backbone, fragmenting the protein into its constitutive parts and eliminates its bioactive function. To avoid this, significant efforts have been made to package the protein therapeutics within a synthetic carrier to sequester them from serum proteases and improve their stability. The next obstacle is the cell membrane. Protein-based drugs are large macromolecules, and thus are often too large to translocate across biological membranes and bind to an intracellular target. Instead, internalization of these proteins in cancer cells often occurs via endocytic pathways, leading to degradation of the delivered protein in the harsh endosomal and lysosomal environment.

Chemical obstacles are also major threats for protein-based drugs. The first one is pH, which can alter the stability of pH sensitive proteins. This is particularly relevant in cancer where the tumor specific pH can drop by more than 1 unit, reaching approximately 5.5 – 6.5 (Xiaomeng Zhang, 2010). This can result in denaturation and misfolding of proteins, thereby eliminating their biological activity. Another common threat are nearby ions. For example, MBLs are well established to interact with Ca^{2+} which can lead to unintended consequences including precipitation, inactivation or toxicity. Finally, high doses of protein given intravenously can also alter their activity as many proteins tend to aggregate at high concentrations (Melanie Hofmann, 2016).

These challenges have created an urgent need for new delivery strategies that can: 1) efficiently encapsulate protein therapeutics; 2) improve stability of the biologic cargo during systemic circulation; and 3) afford preferential delivery to tumor tissue, and enhance their cytoplasmic delivery in cancer cells. Below, I describe the development of a novel, bio-inspired nanoparticle that can be used as a carrier for targeted protein delivery, including our newly found lectin anticancer therapeutic candidates.

Nanoparticles-based drug delivery

Nanoparticles are widely used for drug delivery applications because of their ability to encapsulate large concentrations of therapeutics and selectively deliver them to the diseased tissues (Borm, 2008). With respect to their loading potential, nanoparticles can carry large concentrations of therapeutics due to their large surface to mass ratios. Here, therapeutics are either encapsulated within the core of the particle, covalently attached to the particle surface, or physically adsorbed to the carrier. This strategy allows the nanoparticle carrier to protect drugs until they reach diseased tissues, and controllably release the agent to the target cells. As a result, nanoparticle based therapies can improve the therapeutic activity of loaded cargo while minimizing their off-target effects (Lohcharoenkal, 2014).

Based on these unique properties of particle carriers, new nanoparticle-based strategies were developed for the local delivery of anticancer lectins to tumor tissues. To develop this new technology, a number of design criteria were set: 1) The carrier must be able to preferentially deliver the drug to the tumor tissue; 2) Possess low toxicity towards healthy cells; and 3) Improve the therapeutic efficacy of the loaded cargo.

In addition, the nanoparticles should be biodegradable and stable during long term storage. Biocompatibility and biodegradation are particularly important to avoid long term exposure of healthy tissues to a foreign material, as this can lead to chronic inflammatory responses. Moreover,

biodegradative particle clearance allows for control over the release rate of the drug by tuning particle sensitivity to degradation. Finally, nanoparticles are also amenable to aerosol based delivery. Since many proteins can not be inhaled into patients, packaging the biotherapeutic into an aerosolized carrier can allow therapies to be directly delivered to cancerous tissue for the treatment of lung tumors (**Figure 4**). This not only serves to improve therapeutic outcomes, but also circumvents the need for IV injection. Based on these unique properties, here we focus on drug therapy for lung cancer which is the leading cause of death relative to all other cancers and possesses limited efficient cure from chemotherapy.

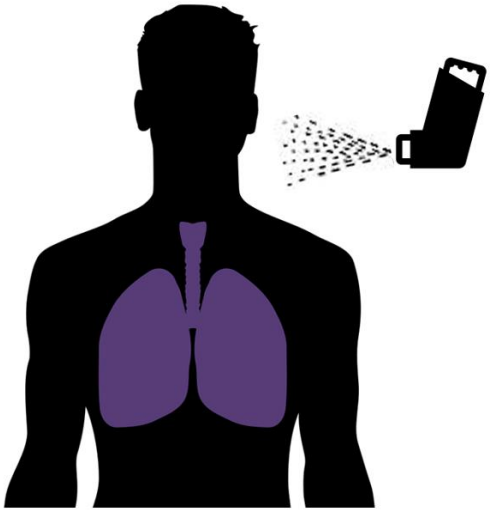

Figure 4. Aerosolized delivery method of the nanoparticles for potential lung cancer chemotherapy. Figure with permission from Andrew Simonson.

Lung cancer therapy

Lung cancer is a leading cause of cancer related mortality, and accounts for ~14% of diagnosed cancers. In 2017, lung cancer killed 155,870 people in the United States (American Cancer Society, 2017). Current lung cancer therapies include surgery, radiation, chemotherapy with cytotoxic drugs, and targeted biotherapeutics. While recent advances in oncology, particularly precision antibodies, have

revolutionized patient care, many of these therapeutic modalities are limited by severe allergic reactions, dangerous side effects and rapid clearance when delivered IV.

Surgery is the most effective procedure, but also the most invasive. There are four types of surgery for lung cancer therapy. These include wedge resection, segmental resection, lobectomy, and pneumonectomy. Wedge resection only removes a small section of lung whereas pneumonectomy removes the entire lung. Even though surgery is highly invasive as the patient's whole or part of the lung is removed, the procedure is very effective because the cancer site is removed as a whole. However, the success cannot be guaranteed because there might be some remaining cancer cells that can lead to recurrence, and the patient may need another surgery again in the future.

Chemotherapy uses chemical toxins to kill cancer cells (Roberts, 2005). Many of the available drugs are cytotoxic agents that act on all dividing cells, cancer or normal. Chemotherapy is required in most cases both after surgery and sometimes before surgery. Several types of effective chemotherapy drugs are available, but all possess side effects. Chemotherapy drugs or anticancer drugs are cytotoxic by exerting their actions on cells either undergoing proliferation or cells at resting phases of the cell cycle. Because anticancer drugs are nonspecific to only cancer cells, side effects thus are attributed from the effect of the drugs on cell cycle of the normal cells as well. Most chemotherapeutic drugs are given through IV injection to allow drugs to travel directly through the circulatory system to reach their target sites. Thus, side effects resulting from off-target distribution of the drug often onset rapidly and are severe. Radiation therapy is quite similar. The procedure uses high-powered radiative energy to kill cancer cells. While effective in treating cancer, inadvertent exposure on nearby healthy cells, or non-cancerous tissues in the beam path, can lead to significant damage.

Recently, targeted drug therapies have reached clinical practice, and offer the hope of selectively killing cancer cells without significant side-effects towards healthy cells. However, these targeted therapies only work in patients with certain types of mutated genes that cause cancers. As a result, targeted drug therapy is most often used in combination with conventional chemotherapeutic drugs.

Interestingly, our newly discovered Lectin 1 shows highly specific killing of certain cancer cells, and thus may represent a novel class of targeted protein onco-therapeutics. Their continued development towards clinical application will require complimentary design of suitable nanoparticle carriers to support their delivery.

Utility of Polylysine and hyaluronic acid for constructing biodegradable nanoparticles

In order to design bioresponsive and biodegradable nanoparticles, we turned to naturally derived polymers. In particular, we sought to exploit electrostatic assembly of bio-inspired cationic and anionic components to form our nanoparticle carrier, as this affords rapid particle production using mild synthesis conditions.

For the cationic component we selected polylysine (**Figure 5a**), which is a bio-inspired cationic polymer made of repeating lysine groups (Park, Jeong and Kim, 2006). Polylysine can be produced by the natural fermentation of bacteria or simple polycondensation. Due to its inherent antimicrobial applications it is used as a food preservative in Japan (Hiraki, 1995). Also, it is commonly used in the tissue culture flask as a coating to improve cell adhesions. These applications indicate that polylysine is generally biocompatible and thus may have utility to form biodegradable and non-toxic particle platforms.

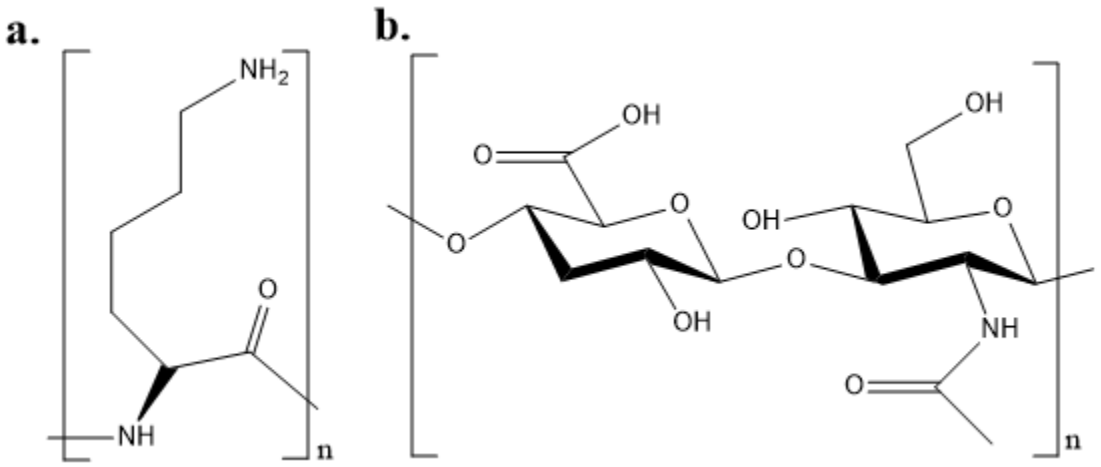

Figure 5. Chemical structures of a. Poly-L-Lysine, and b. Hyaluronic acid

For the anionic component, we selected hyaluronic acid (**Figure 5b**) as it is a negatively charged glycosaminoglycan that is currently FDA approved and established as biocompatible. HA can be found at many locations in the human body, including synovial fluid. It is widely used in cosmetic products as well. Thus, this compound is generally marked as safe.

Since the two materials have positive (PLL) and negative (HA) charges, electrostatic interaction is expected. To explore the potential of these components to electrostatically assemble to form a nanoparticle we next turned to electrospray ionization.

Electrostatic interaction and electro-spraying

Electrostatic interaction is the attractive or repulsive interaction between electrically charged objects. Objects with the same electrical charge will have repulsive interaction while the objects with the different electrical charge will have attractive interaction. Since PLL and HA have different charges, attractive interaction is expected, and thus should be able to form electrostatically complexed materials. To evaluate the ability of these materials to form nanoparticles we turned to electrospray ionization. Electro-spraying works by applying an electric potential to a solution as its passed through a charged

capillary tip. Coulombic repulsion in the spray causes the solution to form a fine nanodroplet mist. Contact of these droplets in a grounded bath solution containing the complimentary cross-linkers allows for rapid assembly of the different components and formation of electrostatic nanomaterials. Here, we applied this approach to spray a solution of HA into a bath of PLL, leading to the rapid formation of PLL-HA gel-like nanoparticles, which we refer to as nanogels, in high yield and low cost (**Figure 6**).

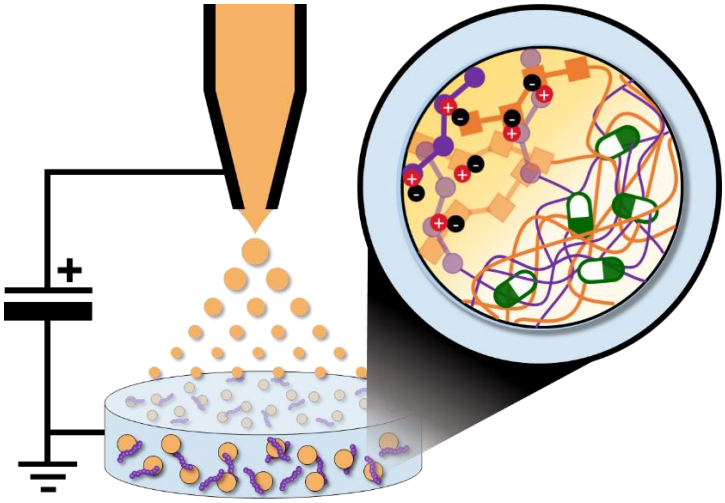

Figure 6. Production of peptide-polysaccharide nanogels by electrospray ionization. The HA solution (orange) is infused through an electrically-charged capillary, resulting in a fine nano-droplet mist that assembles with the PLL (purple) cross-linker to form nanogels.

With the PLL-HA nanogel as the drug delivery carrier and Lectin 1 as the protein-based anticancer drug, we expect to aerosolize the compounds to be used via inhalation in lung cancer patients. The PLL-HA is proposed to protect and deliver lectin 1 to the cancer sites via aerosol delivery to avoid intravenous exposure of the protein cargo. Delivered lectin is expected to effectively kill lung cancer cells with high specificity and low off-target toxicity. In the following chapters I explore the utility of nanogels for drug delivery applications, particularly using the model protein GFP as a surrogate for our lectin protein.

Chapter 5

Materials and Methods

Nanogel particles formulation

The PLL bath solution was prepared by diluting PLL solution to the concentration of 0.01% v/v PLL in 30 mL DI water. The HA solution was made by dissolving 127.8 mg of HA-100K powder in 4 mL DI water. The freshly prepared HA solution then was filtered through the 0.2 um polypropylene syringe filter (VWR; Radnor, PA) and load into the 5-mL syringe. The microneedle was attached. The electro-spray apparatus (Harvard Apparatus; Holliston, MA, **Figure 6**) was set up by having PLL bath grounded while the HA syringe was charged. DC power supply (Spellman High Voltage Electronics; Hauppauge, NY) was used to charge the HA solution at the microneedle with the 24 kV. The charged HA solution was electro-sprayed onto the grounded PLL bath with the flow rate of 0.1 mL/min and 2 mL total volume. The final concentration was expected to be PLL-HA nanoparticle solution with the N-P ratio of 10.

The sprayed solution was incubated in 37 Celsius for 1 hour. The solution was washed one time by DI water using the centrifuge 5430R at 9700 rpm for 30 mins. The washed particle was resuspended in DI water, yielding the free particle solution. The free particle solution was frozen to -80 degree Celsius with the slow-cooling method via isopropanol. The frozen solution was lyophilized with the lyophilizer (Labconco; Kansas City, MO) overnight.

GFP-loaded particle formation

The PLL bath solution was prepared by diluting to the concentration of 0.01% v/v PLL in the 30 mL DI water. GFP of 0.3 mg was dissolved in the PLL bath, yielding the 0.1 mg/mL GFP in the 0.01% PLL solution. The HA solution was made by dissolving 127.8 mg of HA-100K powder in the 4 mL DI water. The freshly prepared HA solution was filtered through the 0.2 um polypropylene syringe filter and load into the 5-mL syringe. The microneedle was attached. The electro-spray apparatus was set up by having PLL bath grounded while the HA syringe was charged. DC power supply was used to charge the HA solution at the microneedle with the 24 kV. The charged HA solution was electro-sprayed onto the grounded GFP-PLL bath with the flow rate of 0.1 mL/min and 2 mL total volume. The final concentration was expected to be GFP-loaded PLL-HA nanoparticle solution with the N-P ratio of 10.

The sprayed solution was incubated at 37 degree Celsius for 1 hour. The solution was washed one time by DI water using the centrifuge 5430R at 9700 rpm for 30 mins. The washed particle was resuspended in the DI water, yielding the GFP-loaded particle solution. All procedures involving GFP were done in dark to prevent the fluorescent degradation due to the extensive exposure to light. GFP resembles the macromolecule proteins. The GFP-loaded particle was used as a model for future Lectin 1 loading potential (**Figure 7a**).

Doxorubicin-loaded particle formation

The unloaded particle in lyophilized form was acquired accordingly to the method in the previous section. The particle was resuspended in 250 µL DI water for each 1 mg of the unloaded particle. Doxorubicin was weighted out with the 1:1 particle: Doxorubicin mass ratio and solubilized in 250 µL DI water for each 1 mg of the unloaded particle. The dox-particle-containing solution was stirred and incubated overnight. Then the doxorubicin particle solution was washed 1 time with DI water. The

washed solution was resuspended in DI water, yielding the Dox-loaded particles solution. Dox-loaded particle resembles the nanoparticle drug delivery carrier for the well-known drug (**Figure 7b**).

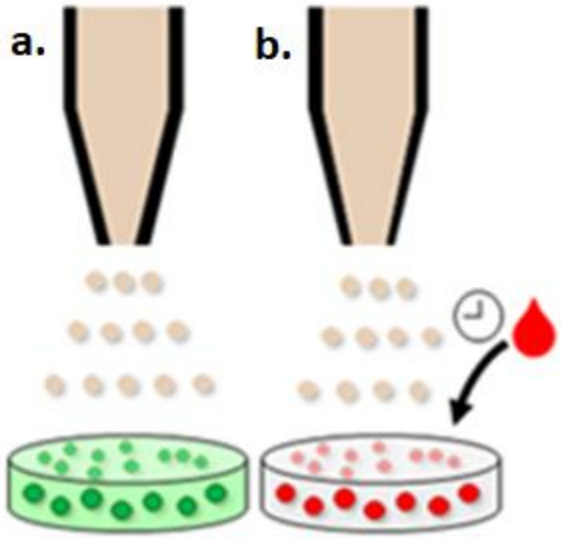

Figure 7. Cartoon for the encapsulation of different molecular cargos in nanogels. a. The model protein GFP (green) is encapsulated by spraying HA into the GFP-containing bath. b. Dox (red) a cancer chemotherapeutic is encapsulated by incubating pre-formed nanogels in a saturated solution of the drug..

Dynamic Light Scattering

Dynamic Light Scattering was used to determine the free particle size. To determine the effect of sonication and the aggregation of particles, the freshly prepared free particles were dissolved in PBS and sonicated with the sonicator (VEVOR; Los Angeles, CA) for 1, 2, 5, and 10 minutes. The aggregation of particles directly alters the size of the carrier. Also, the non-sonicated particle was acquired from the freshly prepared free particle and dissolved in the PBS solution. All conditions were prepared with the particle concentration of 1 mg/mL. Dynamic Light Scattering (Malvern Instruments; Malvern, United Kingdom) was used to determine the size for the particle in each condition using the Z-average. The diameters acquired from Z-average values are compared with other conditions and determine significance by the statistical analysis.

Nanoparticles release study

Multiple therapeutic agents were tested for controlled release with the dialysis method **(Figure 8)**. Prior to the dialysis assay, a small representative sample was acquired from the drug-loaded particles solution. Then the fluorescent intensity of the initial solution was determined by the microplate reader. The fluorescent intensity value was used to determine the initial concentration of the drug-loaded particle and used it to normalize 100% release. The drug-loaded particles in DI water solution were injected into the 300 kDa size dialysis tubing (Spectrum Laboratory; Rancho Dominguez, CA). The dialysis tubing was submerged in PBS with the volume of 30x the dialysis tubing solution. For each time point, samples from multiple locations in the PBS bath were collected and read with a microplate reader. The GFP-loaded particle experiment was read with the fluorescent of 488 nm excitation and 510 nm emission. The Doxorubicin-loaded particle experiment was read with the fluorescent of 480 nm excitation and 560 nm emission. The selected time points were 30 minutes, 1 hour, 2, 4, 24, 48, and 72 hours. The PBS bath solutions were taken at the moment the dialysis tubing was submerged and used as a background control.

For each fluorescent substance, the concentration for each respective fluorescent intensity was calculated from the equation from its respective calibration curve. Then the concentration at each time point was normalized into release percentage and plotted into the graph to visualize the release profile for each drug-loaded particle. The release profile curve should tell us how fast the drug will be released in the PBS solution. The normalized equation used is as followed;

$$\%\, Release\ (time) = \frac{Concentration(time) - Background}{Concentration\ (Initial\ Solution) - Background} * 100\%$$

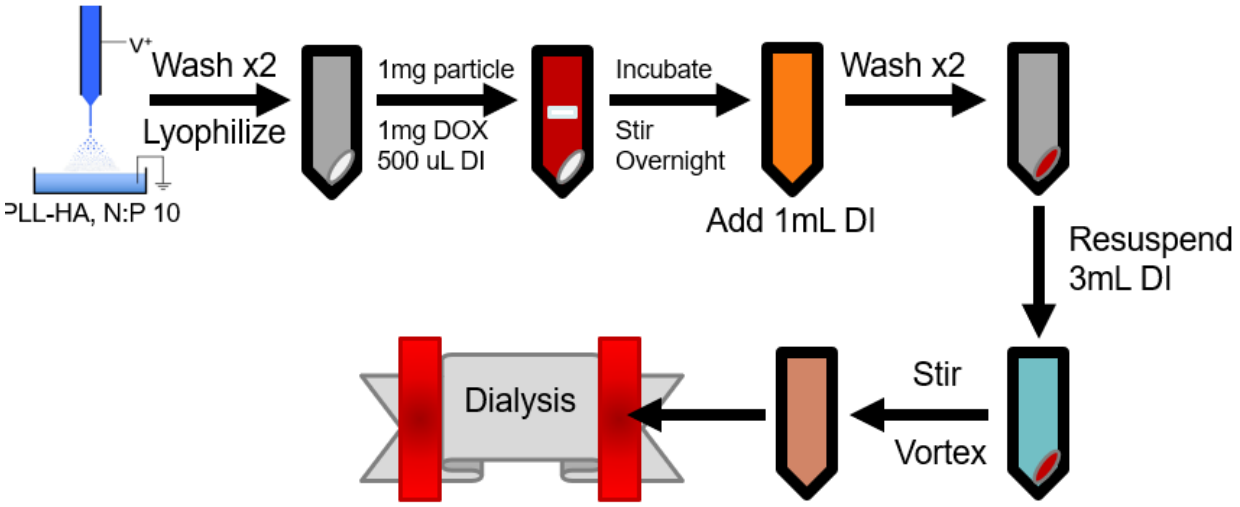

Figure 8. Schematic representation of nanogel preparation, drug loading and release experiment. Dox shown as a representative example.

Dox cytotoxicity assay

The doxorubicin-loaded particle was acquired accordingly to the methods shown above. A549 was seeded on the 96-well plate with the concentration of 2000 cells/well and 100 uL/well of complete RPMI-1640. The seeded cells were incubated in 37 degree Celsius and 5% CO2 for 24 hours. The treatments were concentrated by the concentrator (Labconco, Kansas City, MO) to the desired concentration. The concentration of doxorubicin in the particle solution was determined by the fluorescent intensity from microplate reader and its corresponding calibration equation. The doxorubicin-loaded particle concentrations were achieved by serial dilutions with the dilution factor of 10. The desired concentration was correlated to the IC50 of the free doxorubicin drug at 24 hours. Free doxorubicin drug solution was made by dissolving doxorubicin in complete RPMI-1640 with the same concentrations of doxorubicin in the nanoparticles determined previously.

The supernatant was removed before the treatments. One hundred microlitres of the treatment solutions were added to each well. The negative control was made by the complete RPMI-1640. The positive control contained 20% DMSO in the complete RPMI-1640. The treated cells were incubated for 24 hours. Then the treated supernatant was removed and 100 uL of the 0.5 mg/mL MTT in complete RPMI-1640 solution was added to each well. The MTT-treated cells were incubated in 37 degree Celsius and 5% CO for 2 hours. After that, the MTT-containing supernatant was removed then the spectrophotometric-grade DMSO was added to each well. Finally, cells were incubated for another 15 minutes in 37 degree Celsius. Then the 96-well plate was read by microplate reader at 540 nm.

The highest concentration of the cells wasn't treated with the MTT solution in the previous method. However, its supernatant was removed and replaced with fresh complete RPMI-1640 media. The cells were incubated in 37 Celsius and 5% CO2 for another 72 hours. This would show if there is any small amount of survivor from the Doxorubicin treatment by letting them grow again. After 3 hours, MTT assay was performed accordingly to the protocol above

Cell imaging for GFP-loaded particles interaction

GFP-loaded particles were formulated as described previously. The A549 cell lines were treated with the GFP-loaded particle at the therapeutic concentration. Furthermore, the free GFP and the HA at the maximal concentration before toxicity at the corresponding concentration were used to treat the A549 cells. The treated cells were incubated in 37 degree Celsius and 5% CO_2. After 72 hours, the treated A549 cells were fixed and permeabilized then stained with DAPI and Transferring Red after the supernatant was removed. Then the stained cells were washed with PBS to remove the remaining staining agents and the leftover unbounded GFP. The washed cells were imaged by the confocal microscopy FluorView 1000 (Olympus; Tokyo, Japan).

Statistical analysis

For cell cytotoxicity assays, the data was presented as mean ± SD from at least three independent experiments. Difference between 2 groups was determined using *t* -test with 2-tails assuming unequal variances. The difference of mean among multiple concentrations of the treatments was determined by ANOVA followed by Dunnett's test. The level of significance was determined as $p < 0.05$.

For the controlled release experiments, the data was presented as mean ± SD from at least three independent runs.

Chapter 6

Results – peptide-polysaccharide nanogel carrier for targeted drug delivery

Characterization of the Nanogels

After the electrospray, the nanogels were rapidly formed with an average diameter of ~120 nm **(Figure** 9a). During electrospray the collecting bath quickly turned turbid which indicates the rapid formation of particles, which remain collodially stable in bulk solution (**Figure 9b**).

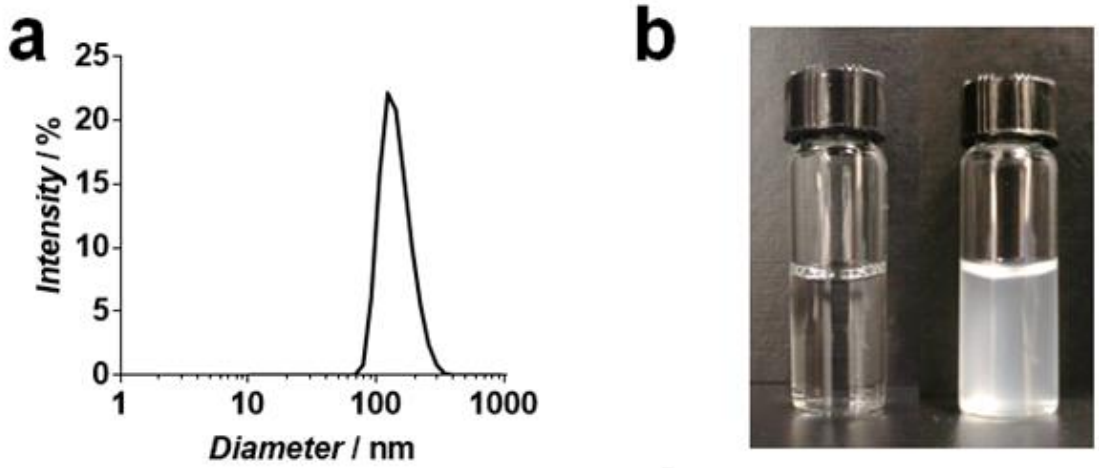

Figure 9. (a) Dynamic light scattering Z-Ave distribution, (b) Visual observation of the nanogels after electrospray.

Drug release from nanoparticles

Doxorubicin-loaded nanogels show a gradual release profile which successfully completed to 100% release after 48 hours. Conversely, the model GFP protein remained encapsulated within the particle for approximately 24 hours, before rapid release between 24 – 48 hours (**Figure 10).** This release profile closely matched the swelling and degradation behavior of these particles (data not shown). This suggests that loaded proteins are retained within the carrier as they swell in physiologic conditions, and release the protein cargo once the particle has completely degraded.

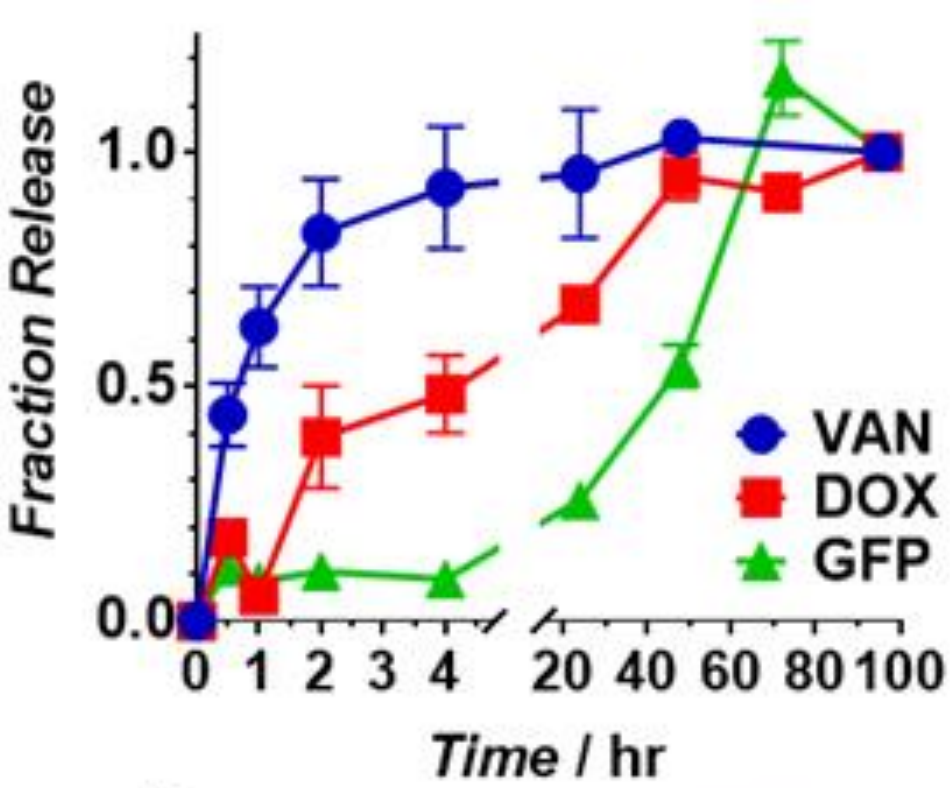

Figure 10. Release profile of the Doxorubicin-loaded NPs *figure will be changed to Dox+GFP only.*

Release Dox cytotoxicity study

The A549 viability plots (**Figure 11**) were created after the 24 hours treatment of Dox and the Dox-loaded nanogels. At the equivalent Dox concentration, the nanogels increased the potency of Dox toxicity toward A549 cell lines by approximately 10 fold. These results suggest that nanogels are able to preferentially shuttle loaded Dox molecules to cancer cells to enhance the chemotherapeutic potency of the drug.

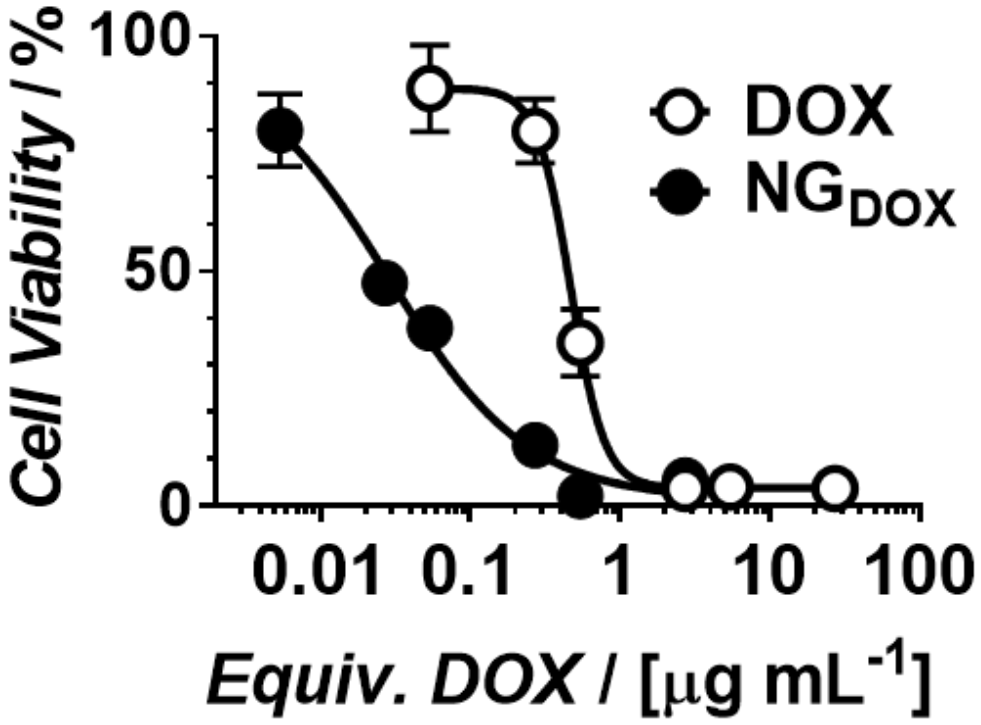

Figure 11. The % Viability of A549 after 24 hours treatment of Dox and Dox-loaded Nanogels

Cell imaging for GFP-loaded particle interaction

Next, we performed fluorescent confocal microscopy on GFP-loaded nanogels to explore their delivery into cells. Images shown in **Figure 12a** show that free GFP was not internalized into treated A549 cells. However, loading of GFP into nanogels led to efficient and rapid uptake into cancer cells, leading to a >11-fold enhancement in intracellular GFP (**Figure 12b**). To evaluate the contribution of HA to the endocytic uptake of the particles, which has previously been shown to mediated cellular particle uptake, we performed similar studies in which GFP-loaded particles were co-incubated in the presence of free HA (**Figure 12b**). This led to a significant reduction in GFP internalization (**Figure 12a,b**) indicating that HA present in the nanogel matrix mediates the cellular uptake of the particles via receptor-mediated endocytic mechanisms.

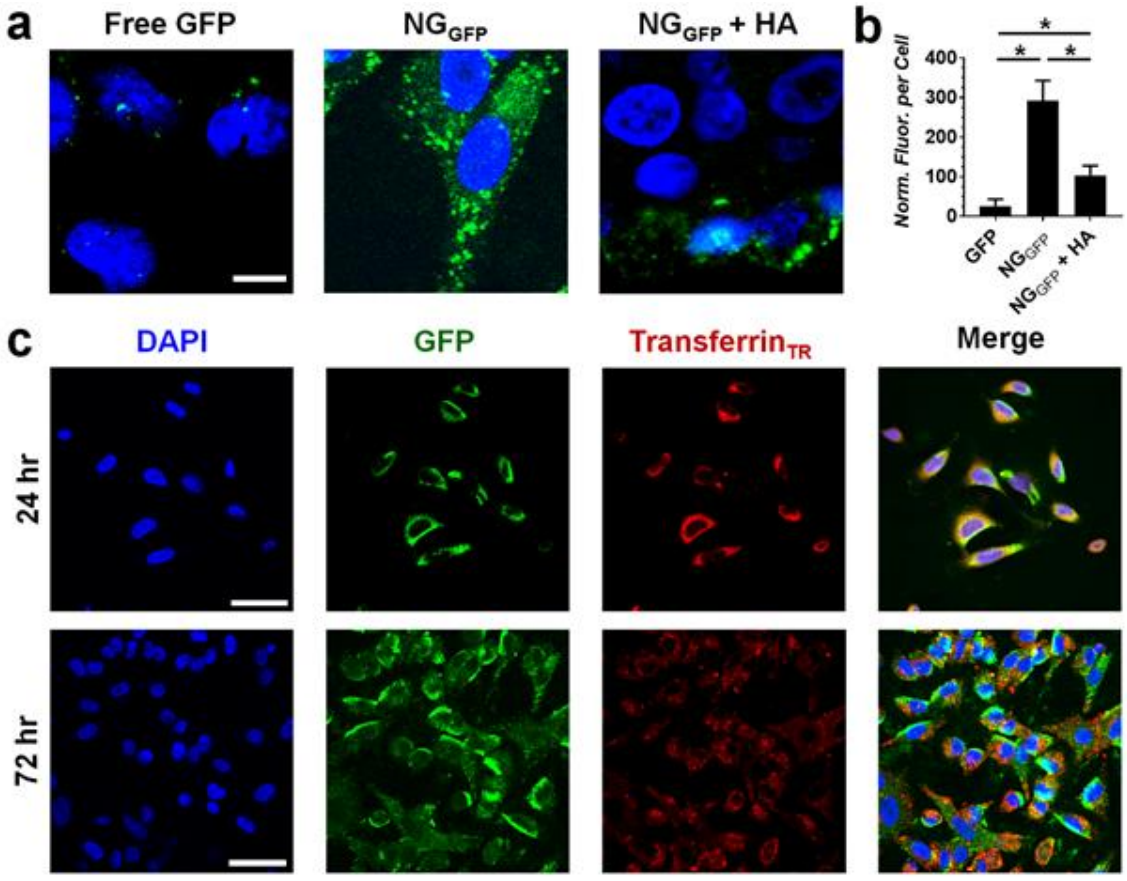

Figure 12. (a) The merged confocal microscopy imaging of DAPI (blue, cell nuclei) and GFP (green). (b) The quantitative values of the average fluorescent intensity for each treatment condition. (c) Confocal microscopy of the A549 treated with GFP-loaded nanogels co-stained with the endosomal marker texas-red transferrin (red).

However, careful inspection of the images in **Figure 12a**, shows that cells treated with GFP-loaded particles show diffuse fluorescence in the cytoplasm. This is counter to the notion of endocytic particle uptake, as we would expect the fluorescent signal only to be observed as punctate endosomes loaded with GFP. This suggests that nanogels are initially internalized via endocytosis, but later escape the endosome to access the cytoplasm. To test this assertion we performed similar experiments in which A549 cells were treated with GFP-loaded particles for 24 or 72 hours, and then co-staine with transferrin to label endosomes (**Figure 12c**). Our results confirm that at early time points (24 hours) nanogels are internalized via endocytosis, as signified by co-localization of GFP and transferrin signals to appear as a yellow/orange color in the merged images. At extended incubation times (72 hours) we observed a release of nanogels into the cytoplasm, characterized by minimal co-localization of green and red signals.

Chapter 7

Discussion

Characterization of therapeutic Lectin for anticancer application

Lectin 1 successfully killed specific cancer cells, including A549, HeLa, OVCAR-3, T24, and CACO-2 cell lines. These cell lines are from the mucosal trait, which possess high glycan content on their surface. Thus, there is more chance of Lectin 1 to bind to the glycan on the surface than other cell lines, including Jurkat and MCF-7, which did not respond to the Lectin 1 treatment. The calculated IC_{50} values from the toxicity study also suggests that the Lectin 1, at the highest potency, was more toxic toward the cancer cells than the traditional chemotherapeutic drug, such as Paclitaxel, by approximately 1000 times in magnitude. Therefore, we are able to decrease the dosage needed for therapeutic uses while increasing the specificity from Lectin 1.

Lectin 1 was non-toxic toward the non-malignant cell, human dermal fibroblast (HDF). As shown in **Figure 2**, the HDF cell lines did not respond to the Lectin 1 treatment at the same therapeutic concentrations. This is very beneficial for the chemotherapeutic application as the Lectin 1 is able to specifically binding and kill the cancer cells from the mucosal trait while leaving the healthy cells alive.

In addition, the optical microscopy snapshots suggests that the Lectin 1 induce cell death by the apoptosis pathway. As you can see from the **Figure 3**, the morphologies of A549 and HeLa cell lines were rounded up and significantly changed it morphology to those of apoptosis indications. The nature of apoptosis pathway is highly beneficial for any drug therapy as toxic/waste substances will be contained in the area of the cells and do not release to the nearby systems.

In conclusion, the Lectin 1 is a very promising future targeted chemotherapeutic agent. However, there are much more to learn about. For example, there need to be a mechanism of action studies to determine if the Lectin 1 does induce apoptosis pathway. Also, *in vivo* studies are needed to examine the stability and activity of Lectin 1 inside the host body.

Development of a nanogel-based vehicle

The nanogels formulation is rapid and high-yield as shown in the **figure 9b.** The entire process takes approximately 3 hours total to get a pure nanogels. DLS data shows that the nanogels diameters were in the 100-300 nm range. This is beneficial for the anticancer drug delivery application as they are residing at the EPR effect range. That being said, the nanogels are expected to passively localize to the cancer site. The DLS also indicates that drug-loaded nanogels possess similar diameter to those free-nanogels.

The release profile of Doxorubicin-loaded nanogels indicates that the small molecule drug was being release overtime from the shell. Furthermore, the nanogels completely release the drug after 48 hours. This is suitable for our therapeutic uses. However, we can modify the release time by adjusting the N:P ratio of the nanogels formulation. At the same time, GFP was retained in the nanogels until 48 hours, suggesting GFP being trapped in the core structure until the material was fully degraded.

The particles release toxicity studies (**Figure 11**) suggest that the nanogels successfully delivered the small molecule drug, Doxorubicin. Also, the potency of the Dox toward A549 was increased by 10 folds with the help of the nanogels. The mechanism of action will be discussed in the next section.

The cell imaging GFP-release studies give us many useful information regarding the Nanogel-assisted intake mechanism of action. Normally, the GFP molecule isn't internalized by the A549 cells. However, with the help of Nanogels, the GFP was internalized. Furthermore, the free HA was added along with the GFP-loaded Nanogels as a competitive study. The result shows that free HA significantly reduce the GFP-loaded Nanogels internalization (**Figure 12a, 12b**). This suggests that the mechanism of action is via the HA influence. From the literature, the receptor, CD44, is for HA as a part of cell adhesion. The HA on the shell of the Nanogels guided the A549 cells to intake the GFP-loaded Nanogels, thus, allowing the GFP intake. With the presence of excess HA, the CD44 binds to the free HA as a competitive inhibitor, thus, significantly reduces the GFP-loaded Nanogels internalization.

Figure 12c indicates the internalization of Nanogels via endocytosis. The GFP was localizing at the endosomes, marked with Transferrin Red at 24 hours. However, the GFP was seen everywhere in the cell cytosols after 72 hours incubation. This suggests that the PLL in the core structure of the Nanogels assisted the endosomes degradation, thus, releasing the contents inside.

In conclusion, the Lectin 1 successfully specifically killed the mucosal cancer cell with high potency. At the same time, we are able to develop the Nanogels-based vehicle to protect, passively localize, and enhance the function of the small molecule and protein-based drugs. However, further studies are needed for the new technology to be deployed. For example, the mechanism of action and *in vivo* studies are needed to examine the activity and stability of the new technology in the real situation. Lastly, we wish that the newly discovered materials will be able to reduce the pain of patients undergoing the chemotherapy procedures with a safer and more efficient tools.

BIBLIOGRAPHY

American Cancer Society. (2017). *Key Statistics for Lung Cancer.* American Cancer Society.

Wim H. De Jong, & Paul JA Borm. (2008). Drug delivery and nanoparticles: Applications and hazards. *Int J Nanomedicine.*, 133-149.

Chen, H. Y. (2014). Biological Toxins and Bioterrorism (ed P. Gopalakrishnakone). *Springer Netherlands*, 1-20.

Elmore, S. (2007). Apoptosis: A Review of Programmed Cell Death. *Toxicol Pathol.*, 35(4): 495–516.

European Food Safety Authority (EFSA). (2008). Ricin (from Ricinus communis) as undesirable substances in animal feed - Scientific Opinion of the Panel on Contaminants in the Food Chain. *EFSA*.

Fraser, IP., Koziel, H., & Ezekowitz, RA. (1998). The serum mannose-binding protein and the macrophage mannose receptor are pattern recognition molecules that link innate and adaptive immunity. *Semin. Immunol. 10*, 363-372.

Frokjaer, S.. (2005). Protein drug stability: a formulation challenge. *Nature Reviews. Drug Discovery*, 298-306.

Hiraki, J. (1995). Basic and applied studies on ε-polylysine. *Journal of Antibacterial Antifungal Agents*, 349-354.

Ishikawa, K. M. (2017). Glycan Alteration Imparts Cellular Resistance to a Membrane-Lytic Anticancer Peptide. *Cell Chemical Biology 24*, 149-158.

Lannoo, N. (2015). J. M. Review/N-glycans: The making of a varied toolbox. *Plant Science 239*, 67-83.

Liu, Z. (2012). Animal lectins: potential antitumor therapeutic targets in apoptosis. *Appl Biochem Biotechnol*.

Hofmann, M., Winzer, M., Weber, C., & Gieseler H. (2016). Prediction of Protein Aggregation in High Concentration Protein Solutions Utilizing Protein-Protein Interactions Determined by Low Volume Static Light Scattering. *Journal of Pharmaceutical Sciences, Volume 105, Issue 6*, 1819-1828.

Oliveira-Ferrer, L., Legler, K., & Milde-Langosch K. (2017). Role of protein glycosylation in cancer metastasis. *Semin Cancer Biol*.

Park, T. G., Jeong, J. H., & Kim, S. W. (2006). Current status of polymeric gene delivery systems. *Advanced Drug Delivery Reviews*, 467-486.

Chabner, B. A, & Robert, T. G. Jr.. (2005). Chemotherapy and the war on cancer. *Nature Reviews Cancer 5*, 65–72.

Lohcharoenkal W., Wang L., Chen Y. C., & Rojanasakul Y. (2014). Protein Nanoparticles as Drug Delivery Carriers for Cancer Therapy. *BioMed Research International*.

Zhang, X., Lin, Y., & Gillies, RJ. (2010). Tumor pH and its measurement. *J Nucl Med*, 51(8): 1167–1170.

Academic Vita of Atip Lawanprasert

Axl5376@psu.edu

Education: B.S. from the Pennsylvania State University
Major(s): Biomedical Engineering with Biomaterials option.
Honors: Biomedical Engineering

Thesis Title: CHARACTERIZATION OF ANTICANCER LECTINS AND DEVELOPMENT OF NANOGEL-BASED CARRIERS FOR THEIR TARGETED DELIVERY

Thesis Supervisor: Scott H. Medina, Ph.D., Jian Yang, Ph.D.

Work Experiences

Research Project – Medina's Research Group
Fall 2017 - current
Characterization of Lectin for anticancer application
Collaborating with the Penn State Biology on characterizing the potential anticancer application for the Lectin-based drug.

Bioresponsive Materials for the RNA-delivery
Collaborating with the Penn State Hershey Medical Center on designing and developing a bioresponsive materials for RNA-delivery purpose.

Penn State University (University Park, PA) – Biomedical Engineering
Scott H. Medina, Ph.D.

Research Project – Vogler's Research Group
Summer 2016
Working with professional researchers on developing the understanding of blood coagulation on material surfaces and nanoparticles

Penn State University (University Park, PA) – Material Science and Engineering
Erwin Vogler, Ph.D.

Internship
Designed and conducted experiments on toxicity induced by nanoparticles (including silver, silver-copper, and silver-tin alloy nanoparticles).

National Science and Technology Development Agency (Bangkok, Thailand) – National Nanotechnology Center
Rawiwan Maniratanachote, Ph.D.

Awards:

1. President's Freshmen Award 2015, the Pennsylvania State University

2. President Sparks Award 2016, the Pennsylvania State University

3. The Juniors Evan Pugh Scholar Award 2017, the Pennsylvania State University

Language Proficiency: Thai and English